Kinetics and Mechanism of the Stannous Octoate-Catalyzed Bulk Polymerization of ε-Caprolactone

Robson F. Storey* and John W. Sherman

School of Polymers and High Performance Materials, The University of Southern Mississippi, Hattiesburg, Mississippi 39406

Received June 7, 2001; Revised Manuscript Received December 13, 2001

ABSTRACT: Bulk polymerizations of ε-caprolactone (CL) were conducted at 130 °C, in which the structure and amount of initiator were varied. Polymerization induction periods were observed and attributed to slow heat transfer and to the type of alcohol used as initiator. Induction periods persisted until virtually complete consumption of both ethylene glycol (EG) and 1,3-propanediol (PD). 1-Butanol displayed no detectable induction. ^{1}H NMR suggested that induction was a result of strong and unique interactions between the diols and stannous octoate, which lead to the formation of more stable, less reactive stannous alkoxides compared to stannous alkoxides derived from the polymer chain end. Only after virtually all free diol was consumed did chain propagation commence at the normal rate. The rate of polymerization was insensitive to the [CL]/[EG] ratios chosen for this study. The results were consistent with a mechanism in which stannous alkoxide initiator is formed in situ via reaction between stannous octoate and alcohol, and stannous alkoxide chain ends are the actively propagating species.

Introduction

Degradable polyester materials based on lactone monomers, including L-lactide, DL-lactide, δ-valerolactone, and ε-caprolactone, are increasingly being considered as replacements for traditional nondegradable thermoplastics. Increasing interest in the synthesis of environmentally friendly materials has caused new scientific interest in understanding the kinetics and mechanism of lactone polymerization, particularly the role of the dominant catalyst used in the reactions, stannous octoate. Stannous octoate (SO) is the catalyst of choice for lactone polymerizations for a variety of reasons, chief among them being its low cost, low toxicity, and high efficiency. Although the first reports of the use of stannous octoate surfaced in the late 1960s,[1] only recently has the true role of the catalyst been revealed.

Controversial reports have appeared in the literature for some time about the nature of SO activity in the polymerization of lactones. Two basic types of mechanisms have been proposed: directly catalytic type,[2−5] where the catalyst serves to activate monomer through coordination with its carbonyl oxygen, and monomer insertion type mechanisms, where the catalyst acts as co-initiator along with either purposely added or adventitious hydroxy impurities, and polymerization proceeds though an activated stannous alkoxide bond.[6−12] Most recently, reports have tended to favor monomer insertion type mechanisms. For example, Penczek et al. have published kinetic results which strongly suggest that SO acts as co-initiator in the presence of an initiating alcohol and that polymerization proceeds only through stannous alkoxide active centers derived from the reaction of stannous octoate with the purposely added alcoholic initiator;[7,8] their specific system involved ε-caprolactone monomer in THF at 80 °C. An additional paper provided direct spectroscopic evidence of tin covalently bound to the polyester chain end.[9] Additionally, Kricheldorf and co-workers have recently published supporting mechanistic work dealing with the interaction of a variety of alcohols and ester/alcohols with

stannous octoate and how the structure of each can effect the strength of catalyst−alcohol interaction.

In this paper, we present evidence that the bulk polymerization of ε-caprolactone conducted at 130 °C, similar to polymerizations conducted in THF at 80 °C, displays the characteristic kinetic features of a polymerization that propagates though an active stannous alkoxide center co-initiated by stannous octoate and purposely added alcohol. We shall also discuss how the choice of initiating alcohol can effect the kinetics of initiation.

Experimental Section

Materials. ε-Caprolactone (CL, a gift from Union Carbide) was dried over calcium hydride (CaH₂), distilled under reduced pressure, and stored over activated 4 Å molecular sieves (Fisher). 1,3-Propanediol (PD, 98%, Aldrich) was dried over anhydrous magnesium sulfate (MgSO₄, Fisher) and activated 4 Å molecular sieves, distilled under reduced pressure, and stored over 4 Å molecular sieves. Ethylene glycol (EG, 99.8%, anhydrous, Aldrich), butanol (BuOH, 99.8%, anhydrous, Aldrich), and CH₂Cl₂ (Fisher) were used as received. Tin(II) bis-(2-ethylhexanoate) (SO, 95%, Sigma) was dissolved in dry toluene (Aldrich), dried over anhydrous MgSO₄ and activated 4 Å molecular sieves, and then distilled in two steps. Distillation at atmospheric pressure removed toluene and any residual water not scavenged by the MgSO₄ as a toluene/water azeotrope. Immediately following the removal of the toluene and water, a vacuum (10^{-3} Torr) was applied, and the temperature was raised to affect the distillation of, first, 2-ethylhexanoic acid and then pure, dry catalyst. The fraction collected at 150−160 °C was dissolved in dry *n*-hexane and stored over activated 4 Å molecular sieves at room temperature prior to use.

Characterization. Structural characterization of materials was performed via routine ¹³C and ¹H NMR spectroscopy. Spectra were acquired on a Bruker AC-300 (300 MHz) spectrometer using 5 mm o.d. tubes and deuterated chloroform as solvent. Sample concentrations were 25% (w/v) for ¹³C NMR spectra while 5% (w/v) for ¹H NMR spectra.

Gel permeation chromatography (GPC) experiments were performed to determine not only molecular weights and molecular weight distributions but also monomer conversion. The GPC system consisted of a Waters Alliance 2690 separa-

Table 1. Molar Ratios and Melt Concentrations of Reactants for Induction Period Analysis

experiment	reaction mass (g)	[CL]:[ROH[e]]:[SO]	[CL] (mol/kg)[d]	[ROH] (mol/kg)	[SO] (mol/kg)
1[a]	25.8	$17.0{:}1.0{:}2.38 \times 10^{-3}$	8.49	5.0×10^{-1}	1.18×10^{-3}
2[a]	25.8	$17.0{:}1.0{:}2.38 \times 10^{-3}$	8.49	5.0×10^{-1}	1.18×10^{-3}
3[a]	26.6	$17.0{:}2.0{:}2.38 \times 10^{-3}$	8.23	9.7×10^{-1}	1.16×10^{-3}
4[b]	25.9	$17.0{:}1.0{:}2.38 \times 10^{-3}$	8.43	4.96×10^{-1}	1.17×10^{-3}
5[c]	25.9	$17.0{:}1.0{:}2.38 \times 10^{-3}$	8.43	4.96×10^{-1}	1.17×10^{-3}

[a] ROH = ethylene glycol. [b] ROH = propanediol. [c] ROH = butanol. [d] Mole of reagent per kilogram of reaction mass. [e] Mole of each particular alcohol.

Table 2. ^{1}H NMR Chemical Shifts of Butanol, 1,3-Propanediol, and Ethylene Glycol in the Presence of Stannous Octoate

[ROH]:[SO[e]] ratio	δ^a of BuOH[b]		δ of PD[c]		δ of EG[d]	
	-OH	CH$_2$	-OH	CH$_2$	-OH	CH$_2$
1:0	1.41	3.66	2.55	3.85	3.37	3.70
1:0.25	2.83	3.68	4.21	3.87	4.72	3.73
1:0 0.5	3.45	3.71	4.72	3.90	5.35	3.78
1:1	4.59	3.75	5.93	3.95	6.95	3.83
1:2	5.49	3.79	7.81	4.01	8.71	3.88
1:4	6.89	3.82	9.54	4.07	11.04	3.98

[a] Relative to internal TMS. [b] Butanol. [c] 1,3-Propanediol. [d] Ethylene glycol. [e] Stannous octoate.

Table 3. Molar Ratios and Melt Concentrations of Reactants for Polymerization Kinetics Experiments

experiment	reaction mass (g)	[CL]:[EG]:[SO]	[CL] (mol/kg)[c]	[EG] (mol/kg)	[SO] (mol/kg)
6	25.17	$17.0{:}0.195{:}2.38 \times 10^{-3}$	8.7	9.98×10^{-2}	1.22×10^{-3}
7	25.35	$17.0{:}0.39{:}2.38 \times 10^{-3}$	8.64	2.0×10^{-1}	1.21×10^{-3}
8	25.8	$17.0{:}1.0{:}2.38 \times 10^{-3}$	8.49	5.0×10^{-1}	1.18×10^{-3}
9	25.8	$17.0{:}1.0{:}1.19 \times 10^{-3}$	8.49	5.0×10^{-1}	5.95×10^{-4}
10	25.8	$17.0{:}1.0{:}5.95 \times 10^{-4}$	8.49	5.0×10^{-1}	2.97×10^{-4}
11[a]	25.8	$17.0{:}1.0{:}2.38 \times 10^{-3}$	8.49	5.0×10^{-1}	1.18×10^{-3}
12[b]	25.8	$17.0{:}1.0{:}2.38 \times 10^{-3}$	8.49	5.0×10^{-1}	1.18×10^{-3}

[a] Reaction contains 2.93×10^{-8} mol of H$_2$O. [b] Reaction contains 5.86×10^{-8} mol of H$_2$O. [c] Mole of reagent per kilogram of reaction mass.

tion module, a Waters 484 tunable absorbance detector, an on-line multiangle laser light scattering (MALLS) detector (MiniDawn, Wyatt Technology Inc.), an interferometric refractometer (Optilab DSP, Wyatt Technology Inc.), and two 3 μm PLgel (Polymer Laboratories Inc.) columns connected in series. The system used THF as the mobile phase at a flow rate of 1 mL/min, and sample concentrations ranged from 7 to 10 mg/mL. The detector signals were simultaneously recorded, and the data were converted to absolute molecular weights and molecular weight distributions using ASTRA software (Wyatt Technology Inc.).

Monomer conversion was determined by monitoring the disappearance of the peak centered at elution volume 19.7 mL in the UV detector response (230 nm) of the GPC chromatograms. Experimental monomer concentrations were determined by peak height comparison to a standard UV absorption curve of known CL concentrations and then normalizing to injection concentrations. Ethylene glycol consumption was determined by monitoring the disappearance of the refractive index (RI) response centered at an elution volume of 19.2 mL; the concentration of the initial reaction product between initiator and monomer (1mer) was similarly monitored at an elution volume of 17.9 mL. Peak height, in the case of the EG, was recorded and compared to a standard RI response curve of known EG concentrations and then normalized to injection concentrations. No standard curve could be generated for the intermediate; however, relative concentrations could be calculated on the basis of the normalized peak heights measured in individual GPC experiments.

Polymer Synthesis. *Induction Period Analysis.* The SO-catalyzed polymerizations of CL were carried out neat at 130 °C in 100 mL two-neck, round-bottom flasks (24/40 joints) equipped with one 24/40 rubber septum and one Chesapeake style stirrer bearing plus polished glass stir rod and Teflon paddle. All glassware and needles were dried overnight in an oven at 200 °C prior to use, and all reactions were performed under a dry nitrogen atmosphere in a glovebox. The initiator addition was withheld until the proper polymerization temperature had been reached. Table 1 lists the molar ratios of monomer (CL), initiator (ROH), and catalyst (SO) used in a series of polymerizations designed to investigate the effect of initiator structure on the induction period.

A representative experimental procedure was as follows: to a 100 mL two-neck, round-bottom flask equipped with 24/40 joints was added the SO catalyst solution in hexane (0.5 mL of a 2.49×10^{-2} g/mL solution). The hexane was then removed via a gentle dry N$_2$ purge. The reaction vessel was then placed under vacuum for ~2 min to ensure complete removal of the hexane. After solvent removal, the flask was charged with CL (25 g, 2.19×10^{-1} mol) and then fitted with a stir rod and bearing, a septum, and a thermocouple. The contents were stirred until homogeneous, and then the flask was immersed in a 20 L constant temperature, silicon oil bath at 130 °C. Temperature was monitored as a function of time as the reaction mixture heated to 130 °C, after which the previously warmed initiator (EG, 0.72 mL, 1.29×10^{-2} mol) was quickly injected into the mixture with a 1 cm^3 BD syringe fitted with a BD 18G1$^1/_2$ PrecisionGlide needle. Aliquots were taken after various time intervals by piercing the rubber septum with a 14 gauge stainless steel needle, inserting the needle tip in the melt, and removing an aliquot with a 1 cm^3 BD syringe. The contents were ejected from the syringe into scintillation vials, capped, and allowed to cool. Upon collection of the last aliquot, each aliquot was dissolved in THF to achieve a concentration of approximately 1 wt % for GPC analysis.

Kinetic Investigation. Polymerizations for the kinetic investigation were conducted in the same manner as those in the induction period experiments, except that the initiator was added to the reaction vessel initially. Table 3 lists the molar ratios of monomer (CL), alcohol (EG, PD, or BuOH), and catalyst (SO) used in the polymerizations.

A representative experimental procedure was as follows: to a 100 mL two-neck, round-bottom flask equipped with 24/40 joints was added the SO catalyst solution in hexane (0.5 mL of a 2.49×10^{-2} g/mL solution). The hexane was then removed via a gentle dry N$_2$ purge. The reaction vessel was then placed
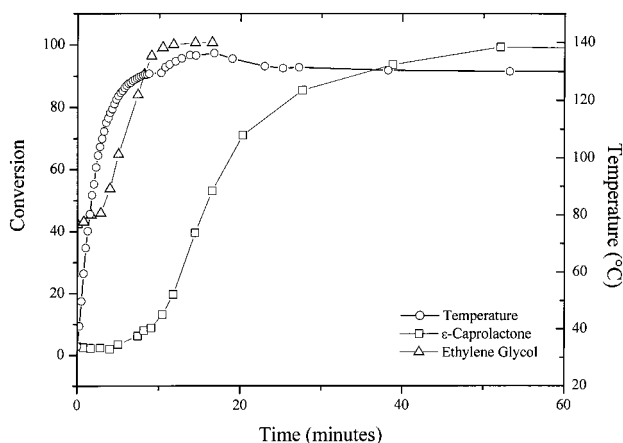
Figure 1. Monomer and initiator conversion and temperature vs time plot for EG-initiated ϵ-caprolactone polymerization; [CL]:[EG]:[SO] = $17.0{:}1.0{:}2.38 \times 10^{-3}$ (experiment 1, Table 1).

under vacuum for ~2 min to ensure complete removal of the hexane. After solvent removal, ethylene glycol was added to the flask (0.800 g, 1.29×10^{-2} mol) followed by ϵ-caprolactone (25 g, 2.19×10^{-1} mol). The reaction vessel was then fitted with a stir rod and bearing, a septum, and a thermocouple. The contents were stirred until homogeneous, and then the flask was immersed in a 20 L constant temperature, silicon oil bath at 130 °C for the appropriate time with continued vigorous stirring. Aliquots were taken after various time intervals as described above.

Results and Discussion

Induction Period Analysis. Figure 1 depicts the conversion vs time plots for both monomer and initiator, as well as the temperature vs time plot of the reaction melt, for an EG-initiated polymerization of CL at 130 °C (experiment 1, Table 1). These data were derived from peak height analysis of GPC chromatograms of aliquots removed from the reaction melt. The data show that about 43% of the initiator was consumed while the contents were still at room temperature. After immersion in the hot oil bath, the rate of initiator depletion was constant but slow for approximately 3 min. During this time, the temperature of the reaction mixture increased to 105 °C, and an additional 3.5% of initiator was consumed. As the temperature increased further, the rate of initiator depletion increased dramatically; however, even after the consumption of EG was well under way 5 min after oil immersion, less than 5% of the total initial monomer concentration had been consumed. Only after 10 min, when ~96% of the initiator had been depleted, did the rate of monomer consumption begin to rapidly accelerate, signaling an end to the monomer consumption lag or polymerization induction period. It is interesting to note that the temperature vs time curve revealed an exotherm upon rate acceleration, due to the slightly exothermic nature of CL polymerization.

Upon first analysis, the polymerization induction period in Figure 1 was attributed to a simple problem of heat transfer. This seemed logical considering that the end of the induction period corresponded directly with the time required to reach the targeted polymerization temperature of 130 °C. However, an earlier publication from our laboratory, which dealt with EG-initiated, SO-catalyzed CL polymerizations conducted at 80 °C, reported the existence of induction periods lasting 30−40 h, although there was no attempt to elucidate their nature.[6] The fact that these induction
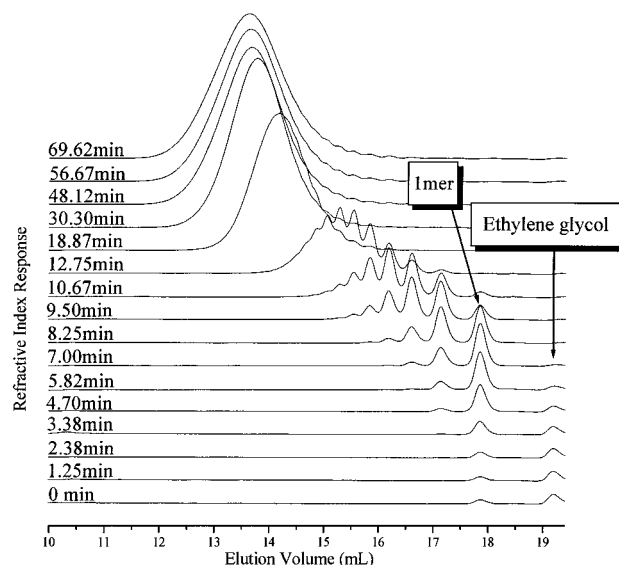

Figure 2. GPC chromatograms of aliquots removed from the reaction mixture of experiment 1 (Table 1); [CL]:[EG]:[SO] = $17.0{:}1.0{:}2.38 \times 10^{-3}$.
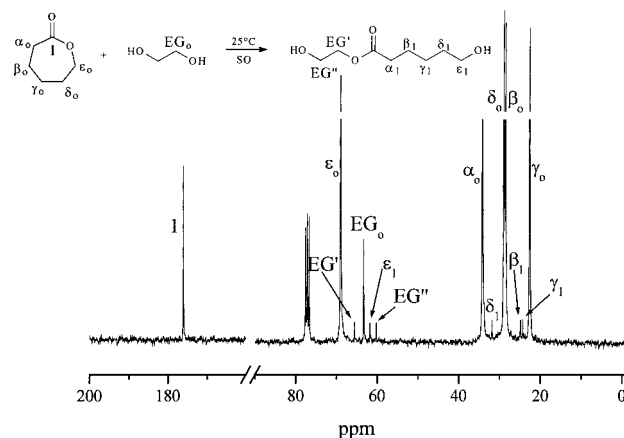

Figure 3. ^{13}C NMR spectrum of the 0 min aliquot of experiment 1, showing the assignments for monomer and (2-hydroxyethyl)-6-hydroxycaproate (1mer) formation.

periods persisted well past the point of thermal equilibration suggests that heat transfer is only partially responsible for the polymerization induction period seen in Figure 1.

Figure 2 shows GC chromatograms of aliquots removed from the polymerization reaction mixture of Figure 1. The data clearly show that the catalyst possesses some level of activity even at room temperature; peak height analysis of the initial (time = 0) GPC chromatogram indicated that approximately 43% of the EG and 3% of the monomer had been consumed prior to oil bath immersion. This represents consumption of approximately the same molar amount of initiator and monomer, suggesting the formation of a 1:1 reaction product. The overlayed GPC chromatograms of Figure 2 show the formation of an intermediate eluting at 17.89 min. ^{13}C NMR analysis of the initial (time = 0) aliquot, shown in Figure 3, indicated that the structure of the intermediate is consistent with the reaction product between one hydroxyl group from EG and one unit of CL, resulting in the formation of 2-hydroxyethyl 6-hydroxycaproate (1mer), or the first product of polymerization. The identification of the 1mer is important because it provided another tool for studying the initiation process, as will be shown later.
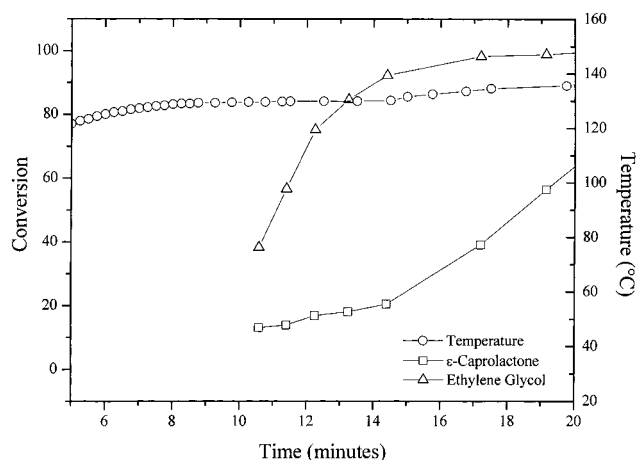
Figure 4. Monomer and initiator conversion and temperature vs time plot for EG-initiated ε-caprolactone polymerization; [CL]:[EG]:[SO] = 17.0:1.0:2.38 × 10⁻³ (experiment 2, Table 1, 10 min delay addition of EG).

Figure 5. GPC chromatograms of aliquots removed from the reaction mixture of experiment 2 (Table 1); [CL]:[EG]:[SO] = 17.0:1.0:2.38 × 10⁻³.

The activity of the mixture at room temperature caused concern that the earlier aliquots, which might be required to stand for up to an hour prior to dilution in THF, might continue to react after cooling to room temperature. Once diluted 100-fold in the solvent, it was assumed that no further reaction would take place. The later aliquots were of less concern since they were diluted sooner upon removal from the melt and were additionally protected against further reaction by crystallization of the polymer upon cooling. To address this concern with the earlier samples, the room temperature reaction was briefly studied. It was found that with a stannous octoate concentration identical to that used in Figure 1, but with a higher initiator concentration (CL:EG ratio = 3:1, mol:mol), the room temperature reaction consumed about 23% of the initiator almost immediately upon mixing. Continued monitoring of the reaction, however, showed that no further reaction occurred, even after 223 h. It was concluded that continued reaction of the aliquots at room temperature was not a concern; however, the room temperature consumption of diol and monomer remains poorly understood and requires further study.

To separate the effects of heat transfer and initiation on monomer consumption, an experiment was conducted where, first, only SO and CL were mixed and heated to 130 °C, followed by addition of the EG initiator. Figure 4 depicts the conversion vs time curves for both monomer and EG as well as the temperature vs time curve for experiment 2, Table 1. Monitoring of the temperature showed that by 10 min the reaction mixture had reached the proper temperature. At this point, a charge of EG was added to the reaction vessel followed immediately by the drawing of aliquots for analysis. Monomer consumption analysis showed that 13% of the CL had been consumed prior to EG addition. It further revealed a pronounced monomer consumption lag even when the reactor was preequilibrated at the proper polymerization temperature. The lag in monomer consumption persisted until greater than 92% of the diol initiator had been consumed. Only then did the polymerization rate accelerate, signaling the end of the induction period. Analysis of diol conversion revealed a conspicuous absence of the consumption lag seen in experiment 1 when EG was added initially. This suggests that the earlier observed induction period in the
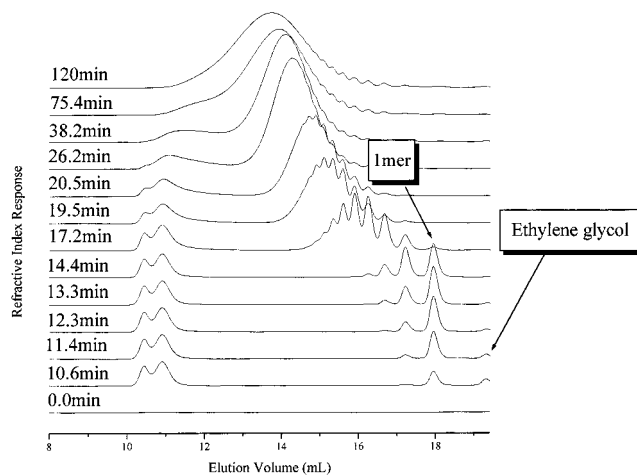
initiator consumption was due to initially low temperature and slow heat transfer into the reactor.

Close scrutiny of the GPC chromatograms of experiment 2, shown in Figure 5, revealed two additional high molecular weight peaks located at elution volumes of 10.9 and 10.4 mL, which were attributed to poly(ε-caprolactone) chains initiated by adventitious water/SO in the absence of EG; this process was responsible for the initial 13% monomer consumption observed at the time of EG addition. Over the course of the experiment, these chains were slowly incorporated into the final polymer distribution via intermolecular condensation and/or transesterification reactions. It is very difficult to rid the reaction of all traces of water, e.g., from glass surfaces or from the extremely hygroscopic SO, unless extraordinarily rigorous vacuum line techniques are used. However, judging by past experience particularly with systems in which water was purposely added (discussed later in this paper and elsewhere[6,12,13]), tin hydroxides and oxides derived from the reaction between SO and water do not compete effectively with tin alkoxides in initiation or polymerization and have only negligible effects on molecular weight provided the water content is sufficiently low.

In another delayed-EG-addition experiment, shown in Figure 6, the amount of EG was doubled, while the monomer/catalyst ratio was held constant (Table 1, experiment 3). Again, the induction period persisted until greater than 95% of the diol had been consumed, at which time monomer consumption accelerated. Interestingly, the duration of the induction period was extended from almost 5 min for experiment 1 (Figure 4) to more than 9 min for experiment 3 (Figure 6). Generally, retardation of polymerization rate in SO-catalyzed lactone polymerizations, at constant temperature, may be attributed to a decrease in the efficiency of the catalyst caused by the presence of either water or 2-ethylhexanoic acid. In the present system neither water nor acid has been added, suggesting that the loss of catalytic efficiency may lie in an interaction of free EG with the catalyst.

Kricheldorf and co-workers have recently illustrated how the structure of the alcohol initiator may influence the strength of the catalyst/alcohol interaction.[4,12] According to these authors, this interaction, in the early stages of reaction, is responsible for formation of the "true" initiating species, subsequent ring opening, and
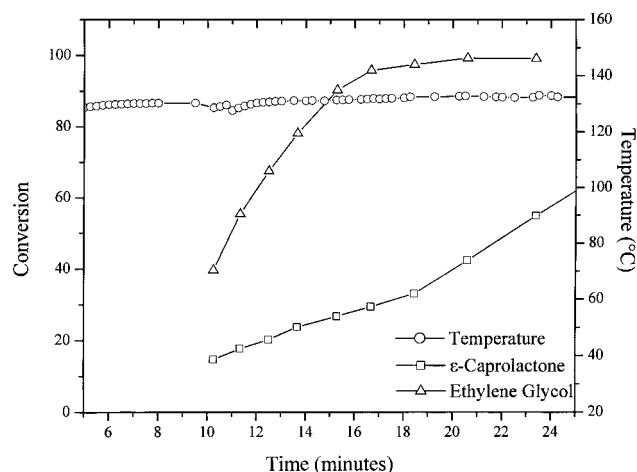
Figure 6. Monomer and initiator conversion and temperature vs time plot for EG-initiated ϵ-caprolactone polymerization; [CL]:[EG]:[SO] = 17.0:2.0:2.38 $\times$ 10^{-3} (experiment 3, Table 1, 10 min delayed addition of EG).

formation of the active, propagating chain end. Prior to the beginning of polymerization, adventitious hydroxy-functional impurities (e.g., water) or purposely added alcohol first complex and subsequently react with SO producing a stannous alkoxide species (**1**) and free 2-ethylhexanoic acid (**3**) as shown in Figure 7, reaction A. Further reaction with a second equivalent of alcohol produces the stannous dialkoxide initiator (**2**) and releases a second equivalent of 2-ethylhexanoic acid (**3**) as depicted in Figure 7, reaction B.[8,12] Adventitious water, meanwhile, serves mainly as a catalyst deactivator via a reversible reaction with **1** or **2**, thereby decreasing the concentration of active initiator and producing a stannous alcohol derivative (**4**), such as shown in Figure 7, reaction C, which is more thermodynamically stable than the stannous dialkoxide and

is less efficient as an initiator.[12] Reaction of **2** with monomer (Figure 7, reaction D) by means of coordination—insertion generates the first actively propagating chain end (**5**, 1mer*) consisting of not only the initiating alcohol fragment but also the active propagating center derived from the first monomer unit and stannous alkoxide. The 1mer* species may either propagate or undergo rapid intermolecular exchange of the stannous alkoxide moiety for a proton from either hydroxyl groups of initiator (if remaining) or another hydroxy chain end, either 1mer or polymeric in nature. This rapid exchange of protons and stannous alkoxide moieties results in a dynamic equilibrium between activated and deactivated chain ends as depicted in Figure 7, reaction E, where R = unreacted alcohol initiator or hydroxy chain ends generated in situ. This process eventually consumes the remaining unreacted alcohol initiator not involved in the initial formation of **2**.

Model reactions, listed in Table 1 as experiments 4 and 5, were conducted using 1,3-propanediol (PD) and 1-butanol (BuOH), respectively, as purposely added alcohol initiator. To probe the effect of alcohol structure on the propagation induction period, the results were compared to a control reaction (Table 1, experiment 3) in which EG was used. Since 1mer generation and consumption are directly related to the rate of ROH consumption as well as the rate of polymerization, monitoring its RI response in GPC chromatograms of aliquots taken during the experiment provides a novel way to monitor any initiation or propagation rate differences induced by alcohol structure. Figure 8 depicts concentration of 1mer, as a percentage of the maximum 1mer concentration, as a function of time after ROH addition to a solution of SO and CL heated to 130 °C. Both diols displayed a slow generation of 1mer, which suggests sluggish initiation. However, generation of 1mer appeared to be finished and con-
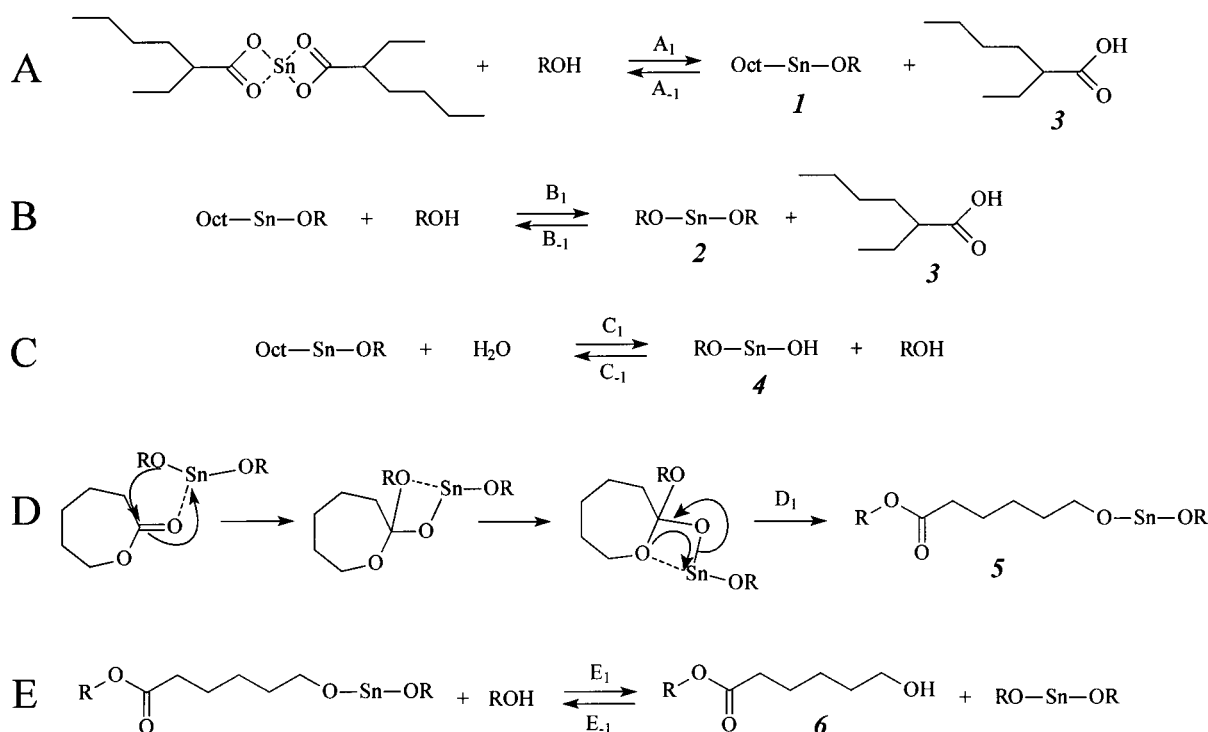

Figure 7. Mechanism of initiation in stannous octoate catalyzed polymerization of ϵ-caprolactone, including (A, B) formation of stannous alkoxide initiator, (C) deactivation of catalyst with reaction by water, (D) coordination/insertion of monomer into the stannous alkoxide bond generating 1mer, and (E) chain transfer of active polymerizing center from 1mer to unreacted alcohol.
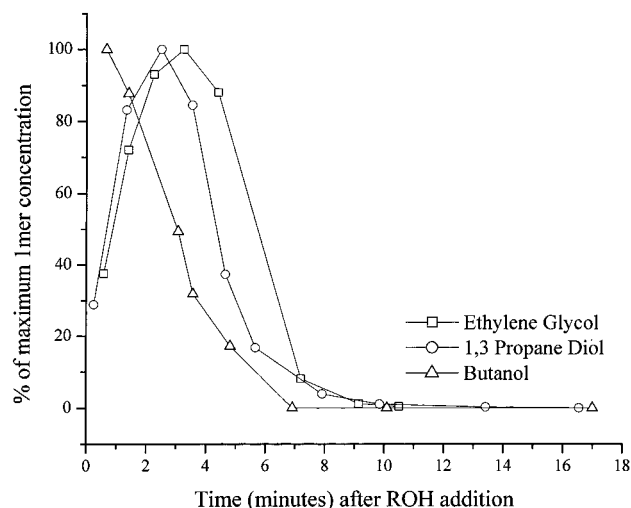
Figure 8. Concentration of 1mer as a function of the original initiator concentration vs time for ε-caprolactone polymerizations utilizing various alcohols as initiator: ethylene glycol, open squares, experiment 2; 1,3-propanediol, open circles, experiment 4; butanol, open triangles, experiment 5.

Figure 9. ^{1}H NMR spectra illustrating the relative downfield shift of alcoholic protons of 1,3-propanediol (1) when compared to 1,3-propanediol in the presence of stannous octoate (1*). [PD]:[SO] = 1:0.25.

sumption well underway in the BuOH-initiated polymerization of experiment 5, suggesting that all of the initiator had been fully consumed even before the first aliquot was taken. ^{13}C NMR (not shown) confirmed that this was indeed the case. The curves in Figure 8 suggest some unique interaction between catalyst and the unreacted diols, which does not exist between BuOH and catalyst, and results in retardation of the initial rate of polymerization.

A series of ^{1}H NMR experiments were conducted, using CDCl$_3$ as the solvent, to investigate the SO complexation behavior of the three alcohols of interest: EG, PD, and BuOH. Earlier experiments by Kricheldorf et al.[4] demonstrated that the magnitude of the proton chemical shifts of both alcoholic protons and methylene protons adjacent to the alcohol moiety in solutions of varying concentration of SO is a good measure of catalyst/initiator interaction. These same authors later suggested,[12] and we believe, that the interaction responsible for the NMR chemical shifts actually consists of an equilibrium reaction between alcohol and SO, with the liberation of 2-ethylhexanoic acid (Figure 7, reaction A). The "alcoholic proton" resonance is therefore the resonance of the combined ROH and octanoic acid protons, which undergo rapid exchange relative to the NMR time scale. Thus, the magnitude of the chemical shift is a measure of the position of the above equilibrium. The results of our experiments, listed in Table 2, showed that each alcohol displays a different affinity for stannous octoate. When butanol was mixed with increasing concentrations of SO, a strong downfield shift of the alcoholic proton from 1.41 ppm (neat butanol) to 6.89 ppm (1/4, mol/mol, BuOH/SO) was observed, as well as an overall downfield shift of 0.16 ppm for the methylene protons α to the hydroxy moiety. This downfield shift in the presence of catalyst indicated that there is, as expected, a strong reaction between the alcohol and SO. The alcoholic protons of the two diols showed even more dramatic downfield shifts in the presence of SO. Those of 1,3-propanediol (Figure 9) shifted downfield from 2.55 ppm (neat) to 9.54 ppm (1/4, mol/mol, PD/SO), whereas those of ethylene glycol displayed an even more impressive downfield shift from 3.37 ppm (neat) to 11.04 ppm (1/4, mol/mol, EG/SO). The down-
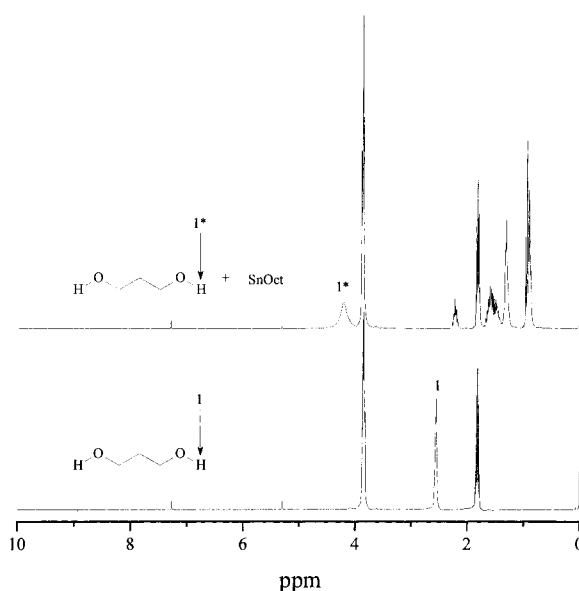
field shifts of the α methylene protons followed a similar trend, with PD displaying an overall shift of 0.22 ppm and EG displaying a more dramatic overall shift of 0.28 ppm. These results showed that the reaction of SO with alcohol follows the trend: butanol ≪ 1,3-propanediol < ethylene glycol.

The extensive reaction of both diols with SO is thought to be similar to ethyl lactate/SO interactions reported by Kricheldorf et al.,[4] where they showed NMR evidence of ethyl lactate behaving as a bidentate ligand in the presence of stannous octoate. Similarly, our results strongly suggest that EG and PD behave as bidentate ligands with both hydroxy groups interacting with a single stannous octoate molecule as depicted in Figure 10, reactions A and B. Because of entropic considerations, the interaction of the monoalcohol with catalyst to form **9** is not as favorable as the interaction with either of the diols. The interaction of EG with SO, to form **7**, is especially strong because the resulting five-membered cyclic complex is kinetically favored compared to the six-membered cyclic complex between PD and SO, **8**.

The differential stability of the stannous alkoxides is most visible, of course, only in the early stages of reaction when there still exists a population of free unreacted alcohol. The more stable the stannous alkoxide produced from the initiator, the more difficult it is for monomer to undergo an insertion reaction to produce 1mer, and the more persistent is the propagation induction period. Insertion of monomer, to form 1mer alkoxide (1mer*), is an irreversible reaction and marks the consumption of 1 mol of initiator. A "consumed" initiator no longer preferentially occupies SO at the expense of propagating chains. As a result, initiation and ensuing propagation occur under two different situations depending on the type of alcohol used for molecular weight control. In one situation, initiator consumption is fast because the first formed stannous alkoxide is similar in reactivity to that derived from the hydroxy functionality provided by ring-opened lactone. Such a situation exists when a monofunctional alcohol is used for molecular weight control. The situation is
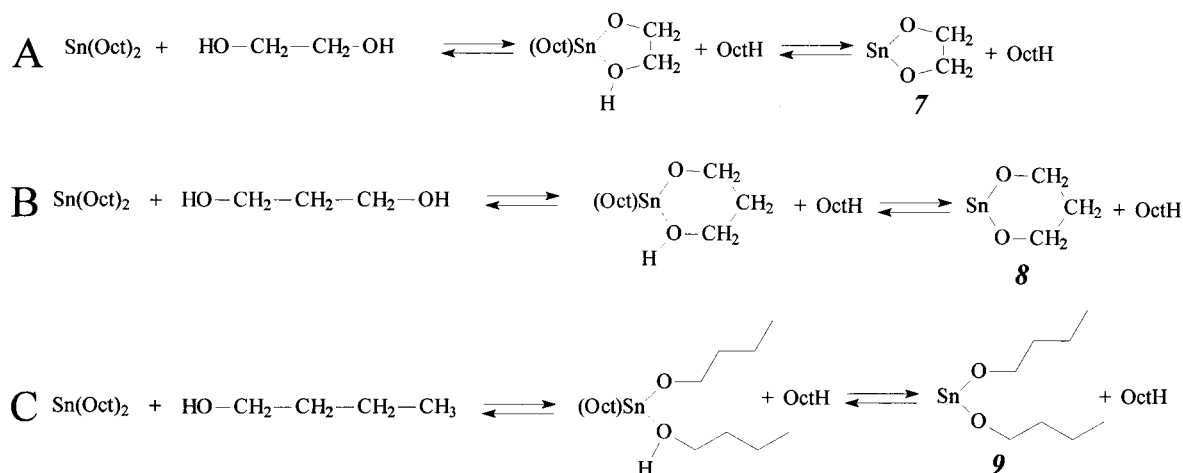
Figure 10. Interaction of stannous alkoxide with a variety of alcohols: (A) ethylene glycol; (B) 1,3-propanediol; (C) butanol.

different when a diol of favorable structure is used. On the basis of the stronger interactions found by ^{1}H NMR, it is apparent that catalyst and EG (or PD) react to form a more stable, less reactive stannous alkoxide than that derived from the ring-opened lactone. Similar stable, cyclic stannous alkoxides were isolated by Kricheldorf et al.,[12] when they studied the interaction of neopentyl glycol and SO. The stronger interaction of diol with catalyst compared to a caprolactone-derived alcohol results in a shift of the equilibrium shown in Figure 7, reaction E (where ROH = diol with favorable interaction with SO), away from the active polymerizing chain end (**5**) to dormant chain end (**6**) where $E_1 \gg E_{-1}$. The resulting starvation of the chain ends for active stannous alkoxide and associated lag in polymerization continue until almost total consumption of diol, at which time the population of more reactive, lactone-derived stannous alkoxide chain ends begins to increase dramatically, as does the rate of polymerization, signaling the end of the induction period.

Kinetics of Polymerization. Discussion of the bulk polymerization mechanism to this point has been limited to initiation. However, during the early stages of polymerization there is a gradual transformation from a system that is dominated by initiation phenomena to a system dominated by propagation of lactone-derived stannous alkoxide chain ends. It is the difference in the nature of the initiation and propagation reactions that is responsible for the observed induction periods. The discussion will now focus on the nature of the active polymerizing chain end and how it effects the overall kinetics of the polymerization.

To gauge the effect of EG concentration on the rate of polymerization, a series of experiments were performed in which the [CL]/[EG] ratio was varied and the catalyst concentration was held constant as shown in Table 3, reactions 6–8. Conversion vs time curves, as shown in Figure 11, were used as a basis of comparison. In each case, polymerization was characterized by an induction period, as discussed earlier, and a propagation rate that was independent of EG concentration. Recently, Penczek and co-workers[7–9] observed similar rate behavior in SO-catalyzed polymerizations of ε-caprolactone in THF conducted at 80 °C. They attributed their result to a propagation mechanism involving monomer insertion at active, stannous alkoxide chain ends. The concentration of active chain ends was proposed to be related only to the initial catalyst concentration and
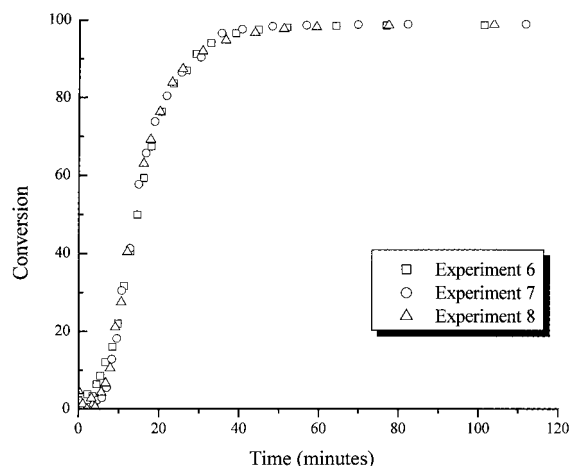

Figure 11. Conversion of CL vs time data for polymerization in which the monomer/catalyst ratio was held constant but the amount of added alcohol was systematically increased: experiment 6, [ROH]:[SO] = 82, open squares; experiment 7, [ROH]:[SO] = 164, open circles; experiment 8, [ROH]:[SO] = 420, open triangles (Table 3).

independent of alcohol concentration provided that [ROH]/[SO] > 2.[8] This minimum excess of ROH, reported by Penczek for solution polymerization and now found by us for bulk polymerization, is a direct consequence of the initiation mechanism depicted in Figure 7, as 2 mol of alcohol is required to fully react with SO to produce the active stannous alkoxide initiator. It also implies that the alcohol–stannous alkoxide equilibria, Figure 7, reactions A and B, are shifted predominantly to the right in favor of the stannous alkoxide. After all stannous octoate has been converted to stannous alkoxide, no additional active polymerizing centers can be created, provided the SO concentration remains constant. Alcohol in excess of [ROH]/[SO] > 2 serves only as a chain transfer agent, generating more chains, but never changing the overall concentration of active chain ends. After initiation, polymerization proceeds as depicted in Figure 12 until complete monomer conversion. The [ROH]/[SO] ratios of experiments 6, 7, and 8 are 82, 164, and 420, respectively, well above the 2/1 ratio required for equivalent rates of monomer consumption. Experimental and theoretical (calculated from the $[CL]_0$/$[ROH]_0$ ratios) molecular weights for experiments 6–8 are listed in Table 4. Good correlation between experiment and theory confirms that alcohol in excess of catalyst concentration serves as chain transfer agent
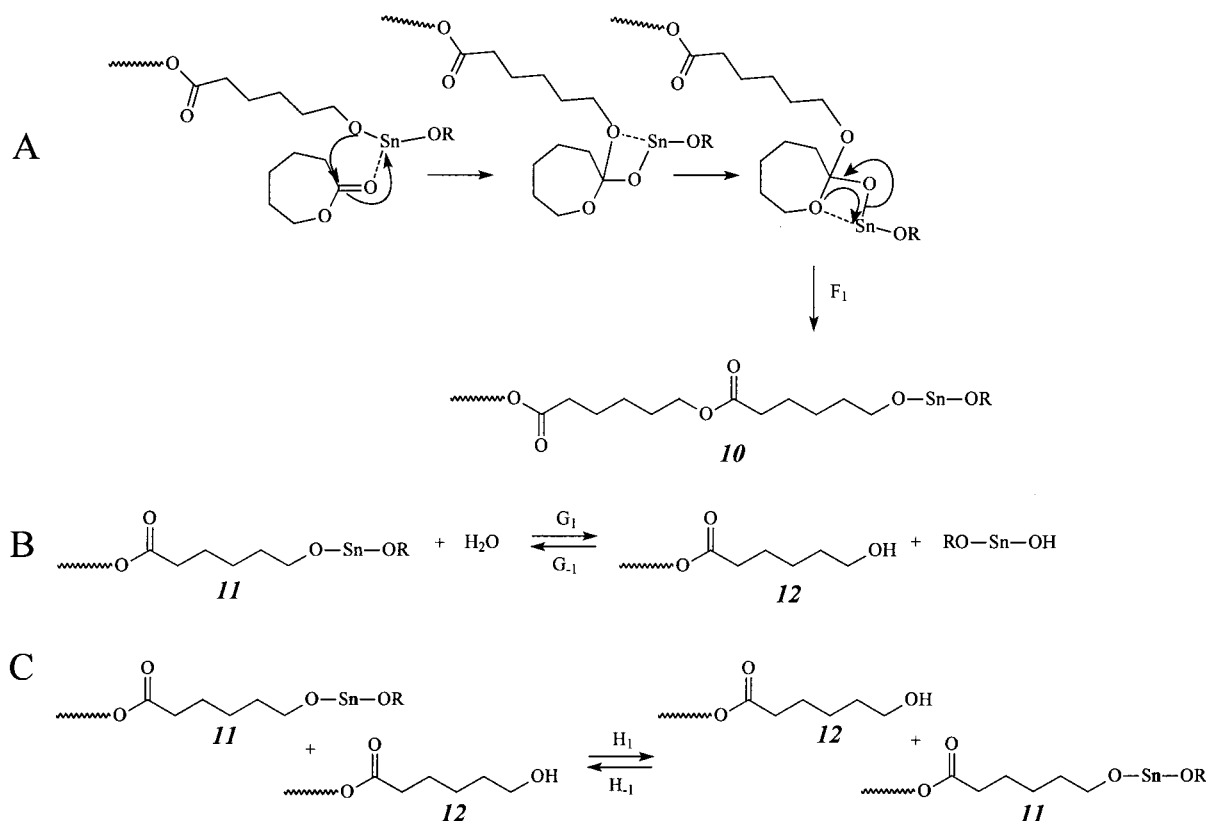
Figure 12. Mechanism of polymerization including (A) chain extension, (B) chain-end deactivation through reaction with water, and (C) intermolecular chain transfer of active chain-end.

Table 4. Molar Ratios and Molecular Weights for Polymerization Kinetics Experiments

experiment	[CL]:[EG]:[SO]	MW[a]	M_n[b]	PDI[c]
6	$17.0{:}0.195{:}2.38 \times 10^{-3}$	9950	10800	1.09
7	$17.0{:}0.39{:}2.38 \times 10^{-3}$	4980	5430	1.12
8	$17.0{:}1.0{:}2.38 \times 10^{-3}$	1940	2240	1.14
9	$17.0{:}1.0{:}1.19 \times 10^{-3}$	1940	2170	1.15
10	$17.0{:}1.0{:}5.95 \times 10^{-4}$	1940	2160	1.12
11	$17.0{:}1.0{:}2.38 \times 10^{-3}$	1940	2240	1.13
12	$17.0{:}1.0{:}2.38 \times 10^{-3}$	1940	2220	1.12

[a] Calculated molecular weight. [b] Experimental number-average molecular weight. [c] Polydispersity index.

and that each hydroxyl group produces one growing chain.

Figure 13 illustrates the dependence of the rate of polymerization on the catalyst concentration in the melt (experiments 8–10). A progressively slower rate of monomer consumption and a related increase in the time required for complete monomer conversion was observed as the concentration of SO was reduced. Again, in each experiment the [ROH]/[SO] ratio was maintained well above the threshold value of 2. Reduction in the initial concentration of SO essentially reduced the overall number of active chain ends in the melt, resulting in lower rates of monomer consumption and, hence, longer reaction times. These results are consistent with a polymerization mechanism whose rate is dependent only on the concentration of stannous alkoxide as outlined in Figure 7. Since only the concentration of instantaneously active chains was reduced in experiments 8–10, and not the overall number of chains as dictated by the alcohol concentration, the experimental molecular weights were predicted to be invariant over these three samples and close to the theoretical value. This was indeed the case as shown in Table 4.
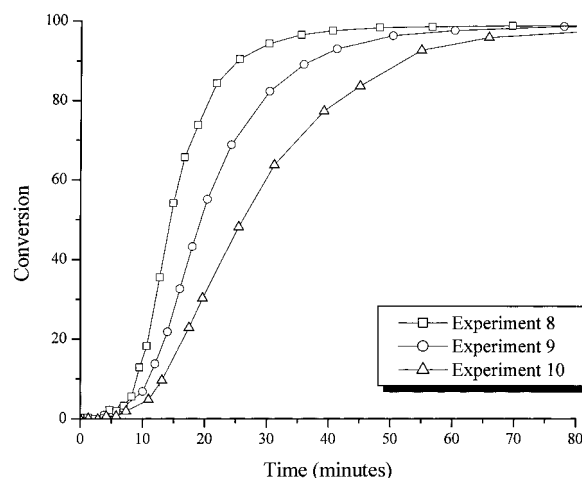
Figure 13. Conversion of CL vs time data for polymerization in which the monomer/alcohol ratio was held constant but amount of added stannous octoate was systematically reduced: experiment 8, 1.4×10^{-4}mol of SO/mol of CL, open squares; experiment 9, 7.0×10^{-5}mol of SO/mol of CL, open circles; experiment 10, 3.5×10^{-5}mol of SO/mol of CL, open triangles (Table 3).

Figure 14 depicts the dependence of the rate of monomer consumption on the concentration of added water. Conversion vs time plots for experiments 8, which contained no added H_2O, and 11 and 12, which contained 2.93×10^{-8} and 5.86×10^{-8} mol of H_2O, respectively, display an increasingly sluggish rate of monomer consumption as the amount of water is increased. As mentioned earlier, the instantaneous concentration of active chain ends may be influenced by the addition of water. As shown in Figure 7, reaction C, a reversible deactivation serves to decrease the
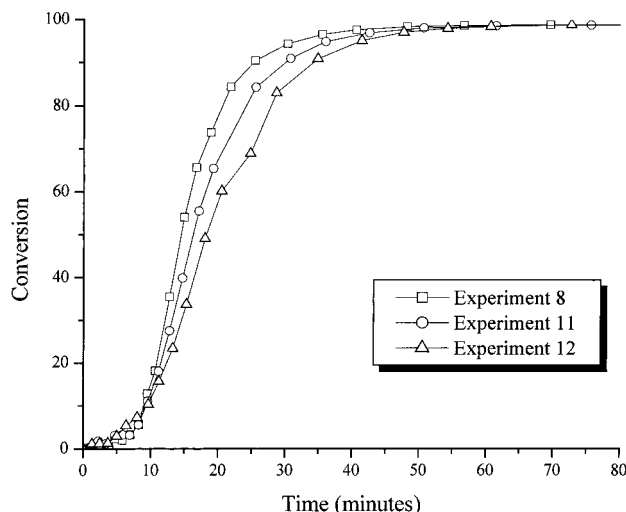
Figure 14. Conversion of CL vs time data for polymerization in which [CL]:[EG]:[SO] = 17.0:1.0:2.38 $\times$ 10^{-3}, but the amount of added water was systematically increased: experiment **8**, no added water, open squares; experiment **11**, 2.93 $\times$ 10^{-8} mol added H$_2$O, open circles; experiment **12**, 5.86 $\times$ 10^{-8} mol added H$_2$O, open triangles (Table 3).

overall number of polymerization centers. This generates a dormant hydroxy end group (**12**), and a stannous hydroxide, which is a much less reactive catalyst and does not actively participate in coordination/insertion in the presence of stannous alkoxide. Stannous alcohol may be reactivated through reaction with 1 equiv of polymer hydroxy chain end, regenerating a molecule of water (reverse of reaction C, Figure 7). Since the addition of water influences only the instantaneous concentration of active chain ends and not the overall concentration of all chains, there was no detectable effect on the experimental molecular weights (Table 4).

Conclusions

The results of the present work illustrate that both temperature and choice of initiator are responsible for propagation induction periods observed in SO-catalyzed, bulk polymerizations of ϵ-caprolactone. Slow heat transfer can contribute to the induction period due to the much lower rates of monomer consumption at lower temperatures; however, competition for SO between the initiating alcohol and the chain end is often also responsible for the lag in monomer consumption. Stannous octoate will preferentially complex and react with alcohols displaying favorable interactions, particularly diols such as EG, allowing the formation of more stable,

less reactive stannous alkoxides, which are responsible for the initial rate lag. After consumption of the free alcohol, all stannous alkoxides derived from ring-opened lactone in the melt show equal reactivity, resulting in the end of induction and the beginning of uninterrupted chain propagation.

The rate of bulk polymerization was found to be insensitive to the [CL]/[EG] ratio, at least in the range of ratios sampled. However, the rate of polymerization was affected by changes in the catalyst concentration as well as the concentration of water added to the polymerization. All results were consistent with the mechanism outlined in Figures 7 and 12 where the active chain end is derived from a reaction between alcoholic chain end and stannous octoate. The results reported here are similar to those for solution-based ϵ-caprolactone polymerizations conducted by Penczek and co-workers.[7-9] The number of overall polymerization sites, therefore, is controlled, in the absence of water, only by the initial concentration of SO provided there is enough alcohol to consume all catalyst. The degree of polymerization is dictated simply by the monomer/alcohol molar ratio. Water acts primarily as a catalyst deactivator, reducing the concentration of instanteously active chain ends.

References and Notes

(1) Schmitt, E. E.; Rohistina, R. A. US Patents 3297033, 1967; 3463158, 1969.
(2) Du, Y. J.; Lemstra, P. J.; Nijenhuis, A. J.; van Aert, H. A. M.; Bastiaansen, C. *Macromolecules* **1995**, *28*, 2124.
(3) Schwach, G.; Coudane, J.; Engle, R.; Vert, M. *J. Polym. Chem., Part A: Polym. Chem.* **1997**, *35*, 3431.
(4) Kricheldorf, H. R.; Kreiser-Saunders, I.; Boettcher, C. *Polymer* **1995**, *36*, 1253.
(5) In't Veld, P. J. A.; Velner, E. M.; van de Witte, P.; Hamhuis, J.; Dijkstra, P. J.; Feijen, J. *J. Polym. Sci., Part A: Polym. Chem.* **1997**, *35*, 219.
(6) Storey, R. F.; Taylor, A. E. *J. Macromol. Sci., Pure Appl. Chem..* **1998**, *A35*, 723.
(7) Kowalski, A.; Libiszowski, J.; Duda, A.; Penczek, S. *Polym. Prepr. (Am. Chem. Soc., Div. Polym. Chem.)* **1998**, *39* (2), 74.
(8) Kowalski, A.; Duda, A.; Penczek, S. *Macromol. Rapid Commun.* **1998**, *19*, 567.
(9) Kowalski, A.; Duda, A.; Penczek, S. *Macromolecules* **2000**, *33*, 689.
(10) Duda, A.; Penczek, S.; Kowalski, A.; Libiszowski, J. *Macromol. Symp.* **2000**, *153*, 43.
(11) Kowalski, A.; Libiszowski, J.; Duda, A.; Penczek, S. *Macromolecules* **2000**, *33*, 1964.
(12) Kricheldorf, H. R.; Kreiser-Saunders, I.; Stricker, A. *Macromolecules* **2000** *33*, 702.
(13) Zhang, X.; Macdonald, D. A.; Goosen, M. F. A.; McCauley, K. B. *J. Polym. Sci., Part A: Polym. Chem.* **1994**, *32*, 2965.